MARTENSITIC TRANSFORMATION IN ZIRCONIUM-NIOBIUM ALLOYS*

S. BANERJEE† and R. KRISHNAN†

Two types of martensite morphologies have been obtained in zirconium and zirconium–niobium alloys containing up to 5.5 wt.% niobium. The massive martensite of pure zirconium and alloys containing less than 0.8 wt.% niobium, shows twin free martensite plates whereas the acicular martensite plates are internally twinned predominantly on $\{10\bar{1}1\}$ planes. Other inhomogeneous shear systems like $\{10\bar{1}1\}\langle\bar{1}\bar{1}23\rangle$ slip and $\{11\bar{2}2\}\langle\bar{1}\bar{1}23\rangle$ twin have also been found to be operative. Evidences for additional inhomogeneous shear inside thick twin bands have also been found. Simultaneous occurrence of both $(\bar{2}112)$ twinning and $(\bar{1}101)$ slip along the common direction $[2\bar{1}\bar{1}3]$ provide another example of multiple shear inhomogeneous deformation. The habit plane determinations of these alloys indicate that the $\{334\}_\beta$ habit, already reported for pure zirconium, remains unaltered with the addition of niobium. This is to be expected because the principal lattice strains do not change appreciably with niobium addition.

TRANSFORMATION MARTENSITIQUE DANS LES ALLIAGES ZIRCONIUM–NIOBIUM

Deux types de morphologie martensitique ont été obtenus dans le zirconium et les alliages zirconium–niobium contenant jusqu'à 5,5% en poide de niobium. La martensite en amas du zirconium pur et des alliages contenant moins de 0,8% en poids de niobium présente des plaquettes de martensite non mâclée alors que les plaquettes de martensite en aiguilles présentent des mâcles internes surtout sur les plans $\{10\bar{1}1\}$. D'autres systèmes actifs de cisaillement non homogène comme le glissement $\{10\bar{1}1\}\langle\bar{1}\bar{1}23\rangle$ et la mâcle $\{11\bar{2}2\}\langle\bar{1}\bar{1}23\rangle$ ont été observés également. Les auteurs ont mis en évidence un cisaillement non homogène additionnel à l'intérieur de bandes de mâcles épaisses. L'apparition simultanée de mâclage $(\bar{2}112)$ et de glissement $(\bar{1}101)$ le long de la direction commune $[2\bar{1}\bar{1}3]$ est encore une preuve de déformation non homogène par cisaillement multiple. Les déterminations du plan d'accolement pour ces alliages montrent que l'accolement $\{334\}_\beta$ observé pour le zirconium pur reste le même après addition de niobium. Ceci était à prévoir puisque les déformations du réseau ne changent pas de façon notable avec une addition de niobium.

MARTENSITUMWANDLUNG IN ZIRKON–NIOB-LEGIERUNGEN

In Zirkon und Zirkon–Niob-Legierungen mit bis zu 5,5 Gew.% Niob wurden zwei Typen der Martensitmorphologie beobachtet. Der massive Martensit in reinem Zirkon und in Zirkon-Legierungen mit weniger als 0,8 Gew.%Niob zeigt zwillingsfreie Martensitplatten; nadelförmige Martensitplatten dagegen enthalten vorwiegend auf $\{10\bar{1}1\}$-Ebenen innere Zwillinge. Auch andere inhomogene Schersysteme, wie $\{10\bar{1}1\}\langle\bar{1}\bar{1}23\rangle$-Gleitung und $\{11\bar{2}2\}\langle\bar{1}\bar{1}23\rangle$-Gleitung wurden betätigt. Außerdem wurden Hinweise auf zusätzliche inhomogene Scherungen im Inneren dicker Zwillingsbänder gefunden. Das gleichzeitige auftreten sowohl von $(\bar{2}112)$-Zwillingsbildung und $(\bar{1}101)$-Gleitung entlang der gemeinsamen Richtung $[2\bar{1}\bar{1}3]$ sind ein weiteres Beispiel für inhomogene Verformung durch mehrfache Scherung. Die Bestimmung der Habitusebenen dieser Legierungen deutet darauf hin, daß die bereits für Zirkon gefundene $\{334\}_\beta$-Habitusebene sich durch Zugabe von Niob nicht ändert. Das wird auch erwartet, weil sich die wesentlichen Gitterverschiebungen durch Zugabe von Niob nicht stark ändern.

INTRODUCTION

Dilute zirconium–niobium alloys have attracted the attention of reactor technologists as a potential substitute for zircaloy-2 for structural use in heavy water moderated reactors. The optimum mechanical properties are obtained when the alloy is in the tempered martensitic structure. As such, interest is centered round the martensitic transformation in this alloy system. Earlier work by Williams and Gilbert(1) has shown that a twinned martensite is formed when the niobium content is greater than 0.6 wt.% Nb while a slipped martensite is formed with lower solute concentrations. Similar observations have been reported earlier by Higgins and Banks.(2)

This investigation presents the observations on a number of Zr–Nb alloys ranging from pure Zr to 5.5 wt.% Nb content. In addition to the general observations on the transition in morphology from massive to acicular martensite, this paper emphasizes the inhomogeneous shear systems that are operative. Determination of the habit plane in both the morphologies has also been carried out.

EXPERIMENTAL

Zirconium alloys containing 0.5, 0.8, 1.8, 2.3 and 5.5% Nb‡ have been prepared from crystal bar zirconium and high purity niobium by electron beam melting. The oxygen contents in these alloys were estimated to be less than 200 ppm. After homogenisation, the electron beam melted buttons were cold rolled to a sheet of about 0.5 mm thick without any intermediate annealing. Small strips from these rolled sheets were sealed in evacuated silica capsules and after a solution treatment of 15 min at 1000°C, the samples were quenched in iced water by breaking the silica capsules.

Specimens for transmission electron microscopy were made from these quenched samples by an initial chemical polishing in HF, HNO_3, water solution followed by an electrolytic polishing at 0°C in acetic, perchloric acid bath, by adopting the window technique.

* Received May 24, 1971.

† Metallurgy Division, Bhabha Atomic Research Centre, Trombay, Bombay-85, India.

‡ All compositions are given in wt.%.

RESULTS

Morphology

Pure zirconium and zirconium–niobium alloys containing up to 0.8 wt.% niobium show a massive morphology, while greater additions of niobium lead to an acicular martensite. Surface relief studies on massive martensites have shown large colonies of parallel platelets. The fine structure of massive martensite as revealed by transmission electron microscopy in iodide zirconium is shown in Fig. 1. The platelet boundaries are not straight and no internal twinning has been observed within the plates. One could notice numerous dislocations within the platelets. The adjacent platelets differ very little in orientation, as no noticeable change in selected area diffraction patterns could be observed, indicating that the platelets belong to the same variant of orientation relation. The boundary between the platelets consists of parallel dislocations (Fig. 2) and single surface trace analysis has revealed that these boundaries appear to correspond to a $\{334\}_\beta$ habit plane, assuming the Burgers[3] orientation relationships to hold good. With increasing additions of niobium, the size of the massive platelets decreases and also the boundary between adjacent platelets gets straightened as can be seen from Fig. 3, corresponding to a 0.8% Nb

FIG. 1. Pure zirconium; β quenched. Transmission electron micrograph showing massive martensite plates with irregular interface between the plates. The small misorientation between the plates has revealed a moiré fringe contrast along the interfaces.

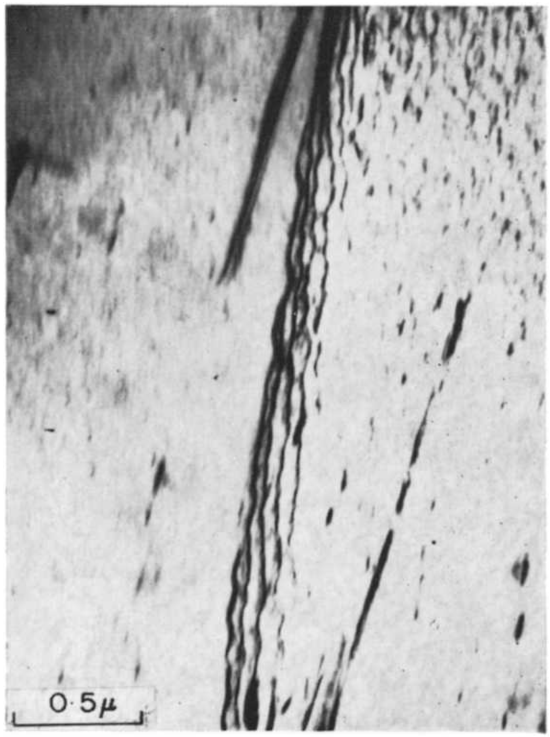

FIG. 2. Pure zirconium; β quenched. The typical dislocation structure at the interface between the massive martensite plates is shown in this micrograph.

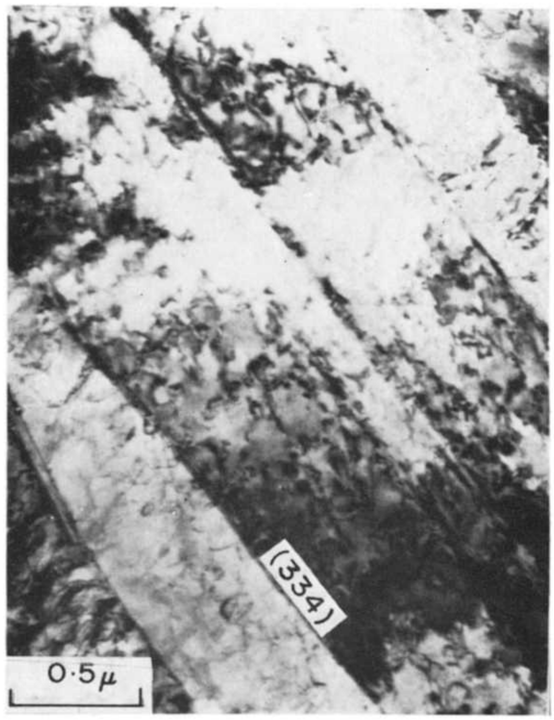

FIG. 3. Zr–0.8% Nb. Micrograph shows smaller dislocated martensite plates with relatively straight interfaces, which correspond to $\{334\}_\beta$ plane. A higher dislocation density in comparison with Fig. 1 is also perceptible.

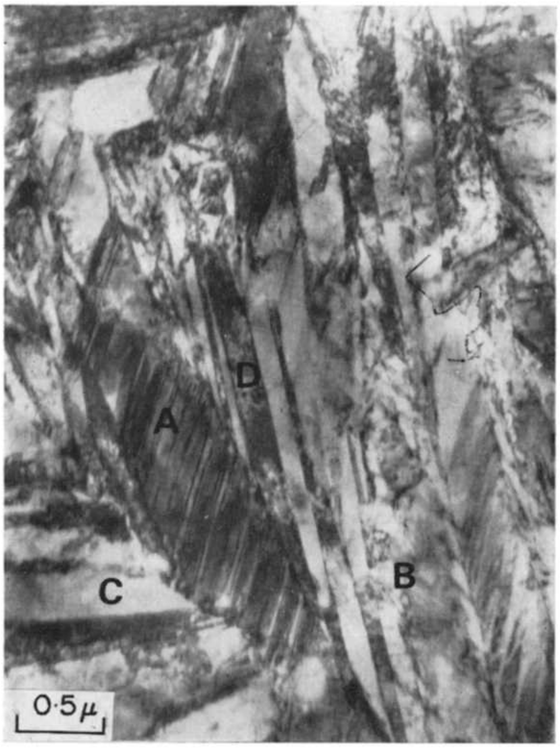

FIG. 4. Zr–5.5% Nb. Acicular martensite structure where internal twinning has taken place inside large primary plates, but the secondary plates, formed in different variants of orientation relation, remain free from internal twins.

alloy. An increase in dislocation density with increasing niobium content is also perceptible (cf. Figs. 1 and 3). Many dislocation tangles within the platelets are seen but no fringe contrast characteristic of stacking faults is visible in these alloys studied.

The acicular martensite of the alloys containing more than 0.8 wt.% niobium, is characterized by a structure consisting of primary martensite plates partioning the parent β grain, and secondary plates subsequently transforming from the partioned β in different variants of orientation relation. It has been observed that the mode of inhomogeneous shear changes with transition in morphology. The acicular martensite plates show predominantly $\{10\bar{1}1\}$ internal twinning. The fraction of the total number of plates that are twinned, increases with increasing niobium content. In general, the primary martensite plates (*A* and *B* in Fig. 4) show internally twinned structure whereas the secondary ones (*C* and *D* in Fig. 4) are not twinned. Similar observation has been made in Ti–Cu martensite.[4] The occurrence of equispaced twins of almost equal thickness in many plates (Fig. 5) and the close correspondence of the measured ratio of the twinned to untwinned portion of plate (Table 1) with the theoretically predicted value of 1:3[2] lead to the conclusion that the twins are transformation twins. The further observation, that internal twinning of primary plates does not appear to result from secondary plate impingement, confirms that these are not deformation twins. Figure 5 shows two distinct appearances of twinned plates. Plate *A* with clear twin matrix boundary shows uniformly spaced $\{10\bar{1}1\}$ twins, the twin plane being more or less normal to the foil plane. In plate *B* the twin plane is steeply inclined to the foil surface, causing those twins to overlap on one another. Hammond and Kelly[5] in Ti–Mn martensite have observed similar effect and termed these as *K* and *L* type martensite plates. According to them these alternately stacked *K* and *L* martensite plates correspond to two variants of orientation relation designated in Bowles–Mackenzie notation as class $A(\alpha+\ \omega+)$ and class $A(\alpha-\ \omega+)$.[6]

Figure 6 shows another platelet which has very thin twins that are lying obliquely to the foil plane. The spacing between the twins being rather large, one could clearly see the individual twins. The platelet boundary is also visible through the projected image of the thin twins.

Internal twinning however is not always as regular as shown earlier. Figure 7 shows twins of varying thickness that are not so equi-spaced. Further, not all

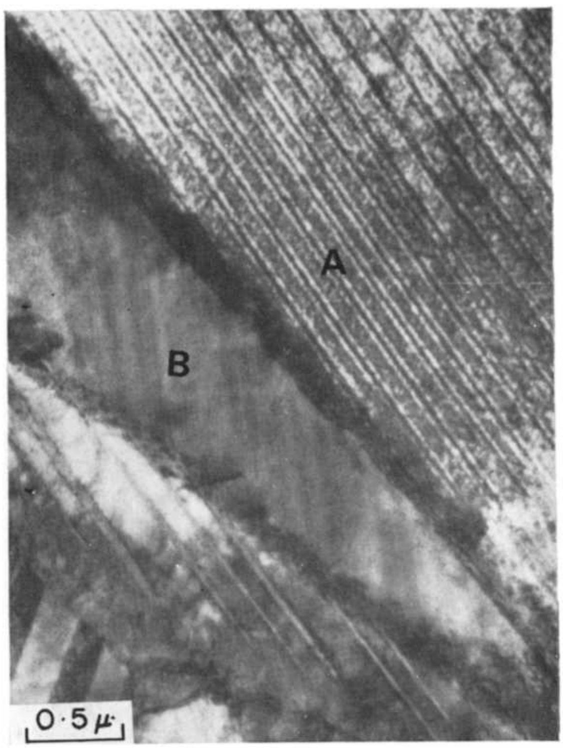

FIG. 5. Zr–2.3% Nb. *K* and *L* type martensite plates showing twins that are near normal and oblique respectively to the foil surface.

Table 1. Morphological Observations and lattice parameters of Zr–Nb Alloys

Alloy composition	Thickness of martensite plates (μ)	Mode of inhomogeneous shear	Ratio of the thicknesses of twin and matrix in a plate	a_0 (Å)	a (Å)	c (Å)	c/a	a/a_0
Pure zirconium	1–2	Slip	–	3.609	3.248	5.198	1.600	0.899
Zr–0.5% Nb	~0.7	Slip	–	3.582	3·232	5.150	1.593	0.902
Zr–0.8% Nb	~0.5	Predominantly slip together with some twinning	1:2.6	–	–	–	–	–
Zr–2.3%Nb	Primary plates ~1.5 Secondary plates ~0.5	Primary plates twinned secondary plates slipped	1:2–1:3	3.577	3.211	5.120	1.594	0.848
Zr–5.5% Nb	Primary plates ~1.1 Secondary plates 0.1–0.3	Predominantly twinned	1:2–1:3	3.568	3.204	5.118	1.597	0.898

The lattice parameters of pure zirconium have been taken from Gaunt and Christian and the parameters for β phase have been obtained by extrapolation of data given in Pearson's *Handbook of Lattice Spacings*. Room temperature lattice parameters have been used for calculation of c/a and a/a_0, since the co-efficients for thermal expansion of the parameters of both α and β phases are close to each other.

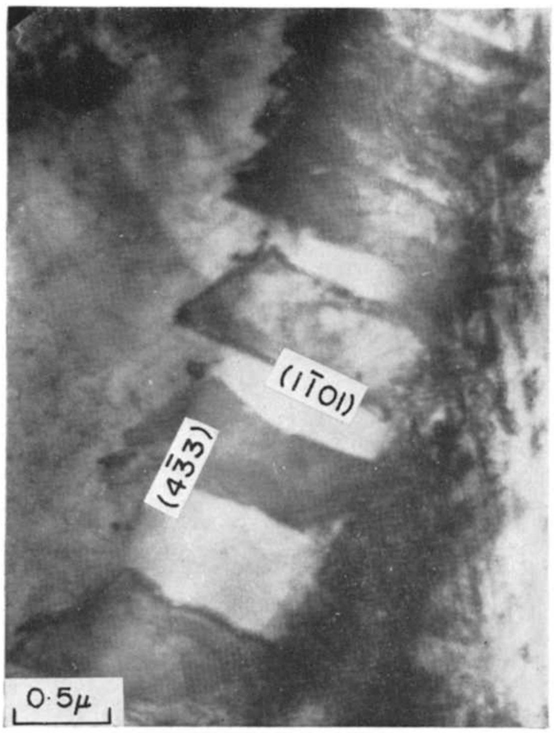

Fig. 6. Zr–5.5% Nb. Thin twins at large spacings between them that are in oblique orientation to the foil plane. The (4$\bar{3}$3) habit has been obtained by considering $(011)_\beta \parallel (0001)_{\alpha'}$ $[11\bar{1}]_\beta \parallel [\bar{2}110]_{\alpha'}$ orientation relation.

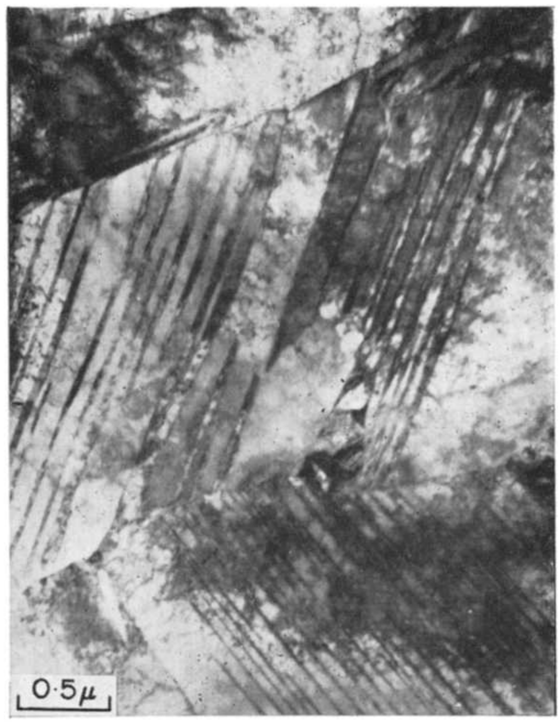

Fig. 7. Zr–2.3% Nb. Micrograph shows formation of step on the interface caused by intersection of twins and the habit plane. The internal twins appear to be non-uniform in contrast with those shown in Fig. 5.

twins are extending from one side of the plate to the other. Also the absence of midribs in the platelets of these martensites is to be mentioned.

Inhomogeneous shear

In the present investigation no attempt has been made to define the plane and direction of the inhomogeneous shear in the massive martensite laths. Dislocations observed in such laths are irregularly arranged to form dislocation tangles, making it impossible to assign any definite plane or direction associated with them. One may even question if the dislocations observed inside the untwinned martensite laths are related at all to inhomogeneous shear,

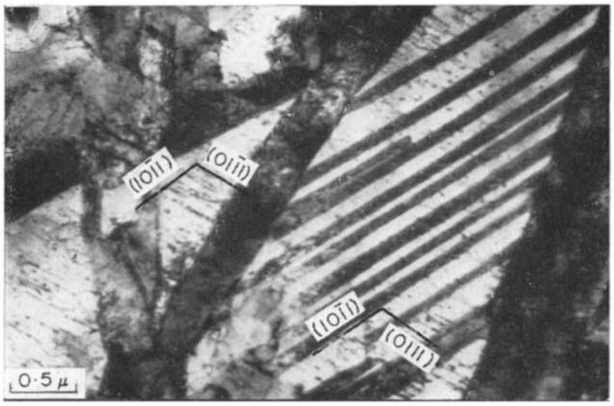

FIG. 8(a). Zr–2.3% Nb. A regular dislocation structure is shown inside individual $(10\bar{1}1)$ twin bands. Trace analysis has pointed out that the dislocations lie along $(01\bar{1}1)$ plane. Habit plane determination has been worked out with $(011)_\beta \parallel (0001)_{\alpha'}$, $[1\bar{1}1]_\beta \parallel [1\bar{2}10]_{\alpha'}$. The dislocated plate shows dislocations lying on both $(10\bar{1}1)$ and $(01\bar{1}1)$ planes.

because in principle such dislocations should be confined to the interface only.

Formation of internal twinning in martensite plates of alloys containing more than 0.8% niobium has facilitated the determination of the exact nature of the inhomogeneous shear. The most predominant shear observed in these alloys is twinning on $\{10\bar{1}1\}$ planes. Figure 8(a) shows a primary martensite plate of zirconium–2.3% niobium alloy internally twinned on $(10\bar{1}1)$ plane. The twinning plane has been determined from the selected area diffraction pattern shown in Fig. 8(b). It is noticed that there is a regular dislocation structure inside the fine twins. The dislocations are parallel to the traces of $(01\bar{1}1)$ plane. The uniform nature of these dislocations in the martensite plate suggests that the dislocations are produced due to a slip type shear contributing to the overall lattice invariant deformation. Though the dislocations associated with the inhomogeneous shear

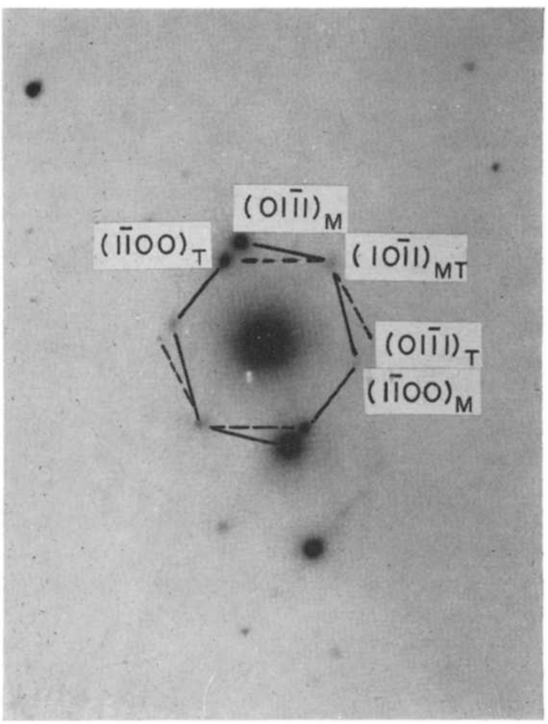

FIG. 8(b). Selected area diffraction pattern showing $(10\bar{1}1)$ twinning.

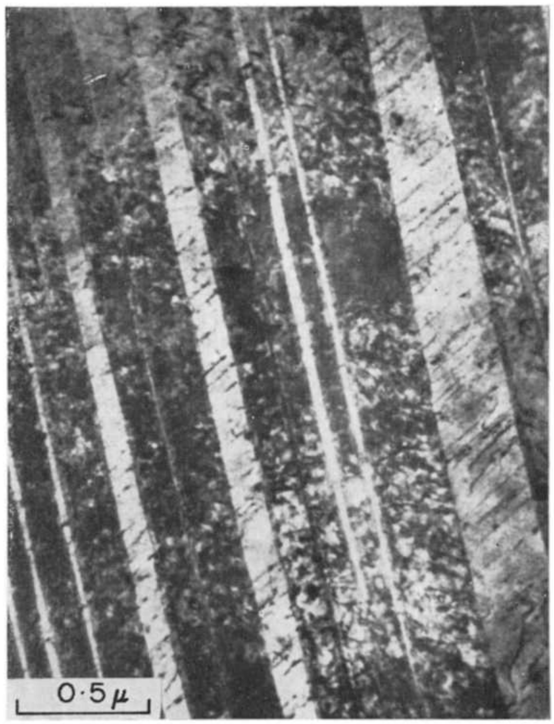

FIG. 9. Another example of regular dislocation structure inside the twin bands of Zr–2.3% Nb alloy.

by slip are expected to be observed only at the interfaces, these dislocations, presumably being the debris of slip on $(01\bar{1}1)$ plane appear in the bulk of the twin band. This observation is not an isolated one and at many places such regular arrangements of dislocations inside the internal twins have been noticed (Fig. 9). Trace analysis has indicated that these dislocations are lying on $\{10\bar{1}1\}$ planes.

Similar arrangement of dislocations are also observed in twin free acicular martensite plates (Figs. 8 and 10). In contrast to the irregular dislocation structure of the massive martensite laths, these plates show the dislocations to be confined to $\{10\bar{1}1\}$ planes. Whereas in Fig. 10 the dislocations

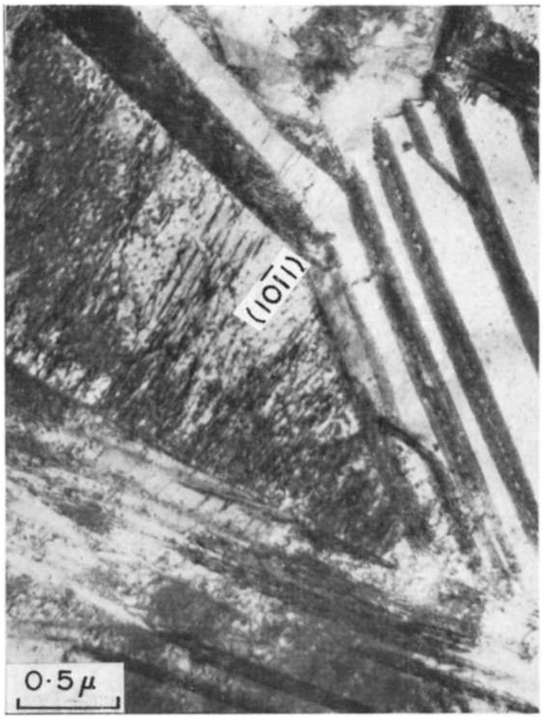

FIG. 10. Zr–5.5% Nb. A dislocated martensite plate showing dislocations lying parallel to (10$\bar{1}$1) plane. Fringe contrast at the twin boundaries are due to the twin lying at an inclination to the foil plane.

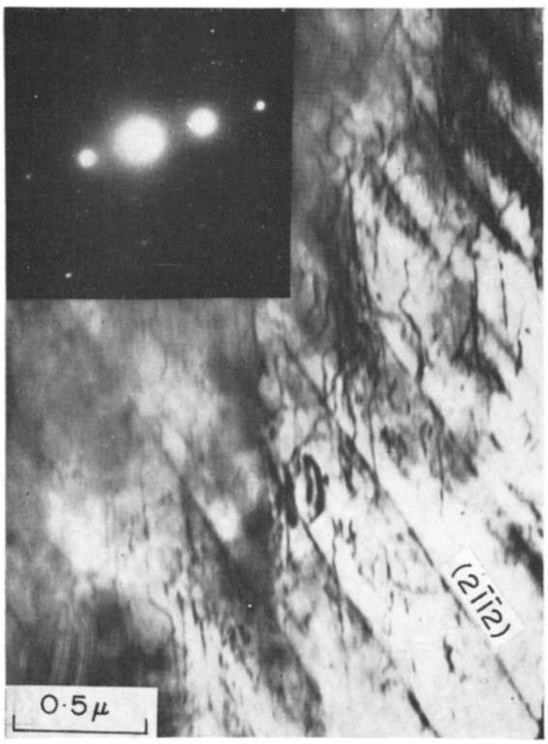

FIG. 11. Zr–2.3% Nb. Fine structure of martensite shows dislocations running through the (2$\bar{1}\bar{1}$2) twin boundaries without getting deviated. Trace analysis indicates that the dislocations are lying on (1$\bar{1}$01) plane and (10$\bar{1}$1) plane with respect to matrix and twin orientations respectively.

appear to be confined to single (10$\bar{1}$1) plane, in Fig. 8 one could observe dislocations to lie essentially in two different directions and trace analysis shows these traces to be parallel to (10$\bar{1}$1) and (01$\bar{1}$1) planes.

The evidence of multiple shear in the martensite plates has also been observed in the structure shown in Fig. 11. The dislocation lines in this micrograph are also lying on (1$\bar{1}$01) plane running across the (2$\bar{1}\bar{1}$2) twin plane, without getting deviated. This is possible only if the slip plane in the matrix is coplanar with

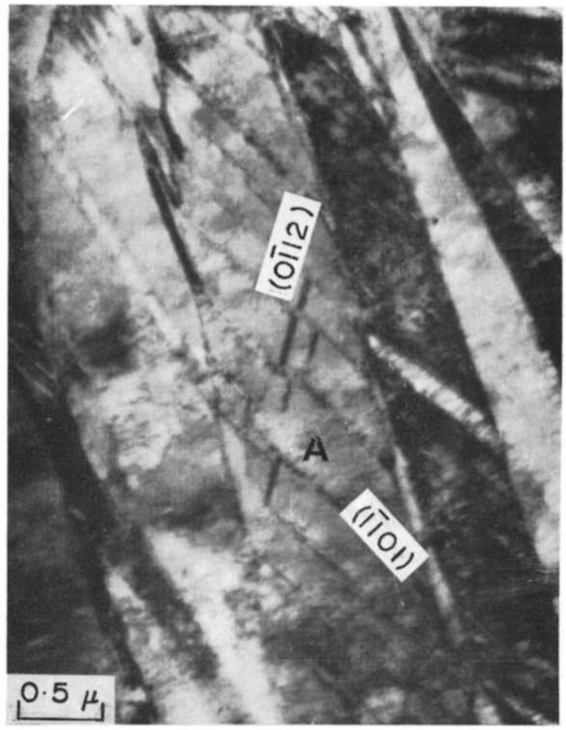

FIG. 12. Zr–5.5% Nb. Micrograph shows twinning on two planes in a martensite plate. Twin spots in selected area diffraction pattern and trace analysis have indicated that the twins correspond to (1$\bar{1}$01) and (0$\bar{1}$12) twin planes. These twins are compatible because the direction associated with (0$\bar{1}$12) twin shear lies parallel to (1$\bar{1}$01) twin plane.

the slip plane in the twinned crystal. The compatibility of these multiple slip systems is discussed later.

In Fig. 12, plate A is twinned on both (1$\bar{1}$01) and (0$\bar{1}$12) planes. The (0$\bar{1}$12) twinning in this case is confined only to the central portion of the plate. Since (10$\bar{1}$2) plane is the common deformation twin plane at room temperature it is possible that the (10$\bar{1}$2) twinning has taken place as a result of the accommodation stresses in the alloy whose M_s temperature is close to the room temperature.

Habit plane

X-ray and electron microscopic investigations have shown that the amount of β-phase retained in these alloys is negligible making it impossible to determine the habit plane directly. Earlier observations in pure zirconium[7] have shown that the lattice correspondence of the parent β and the matrix α' follows the Burgers relation very closely. The same orientation relationship has also been assumed for the zirconium–niobium alloys, since the magnitude of the principal strains involved in the b.c.c. to h.c.p. transformation of these alloys remains almost unaltered. The habit plane determination has been worked out by single surface trace analysis of plate interfaces with respect to α' orientation on a (0001) stereographic projection and then transferring the loci of the trace normals on a (110) projection maintaining the Burgers relation. To minimise the scatter in the determination of habit plane of massive martensite plates, only those plates have been considered which exhibited fairly straight interfaces.

The habit plane corresponding to massive martensite structures has been found to be close to $\{334\}_\beta$ plane without much ambiguity but in case of acicular martensite the loci of trace normals are distributed in such a way that almost all of them are intersecting both (111)–(001) and (111)–(011) great circles near (334) and (344) poles, respectively. However (334) pole has been selected as the habit plane normal because the point of intersections of these loci of trace normals is very near to the (334) pole [1° away from the (334) pole].

Figure 13 is a typical micrograph showing martensite plates belonging to two colonies impinging on each other. The habit planes corresponding to these colonies are $(433)_\beta$ and $(4\bar{3}3)_\beta$. Figure 14 shows another interesting aspect where plate boundary is zig-zag. The formation of steps on the interface is

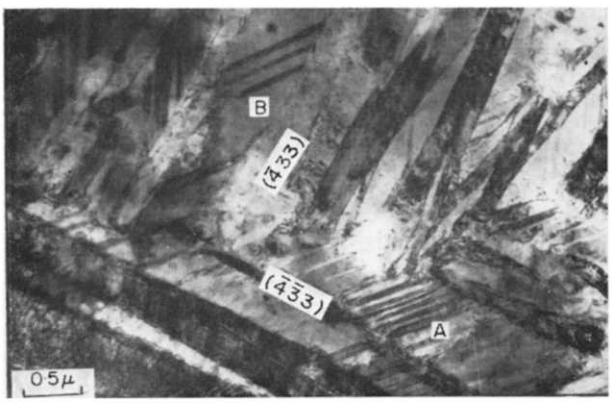

FIG. 13. Zr–5.5% Nb. Martensite colonies of two different habits corresponding to $(\bar{4}\bar{3}3)_\beta$ and μ $(\bar{4}33)_\beta$ planes are shown in the micrograph. The respective orientation relations are $[11\bar{1}]_\beta \parallel [11\bar{2}0]_{\alpha'}$ and $[11\bar{1}]_\beta \parallel [\bar{1}2\bar{1}0]_{\alpha'}$, $(011)_\beta$ plane being parallel to $(0001)_{\alpha'}$ in both the cases. The internal twins in plates A and B are of $\{10\bar{1}1\}$ and $\{11\bar{2}2\}$ types, respectively.

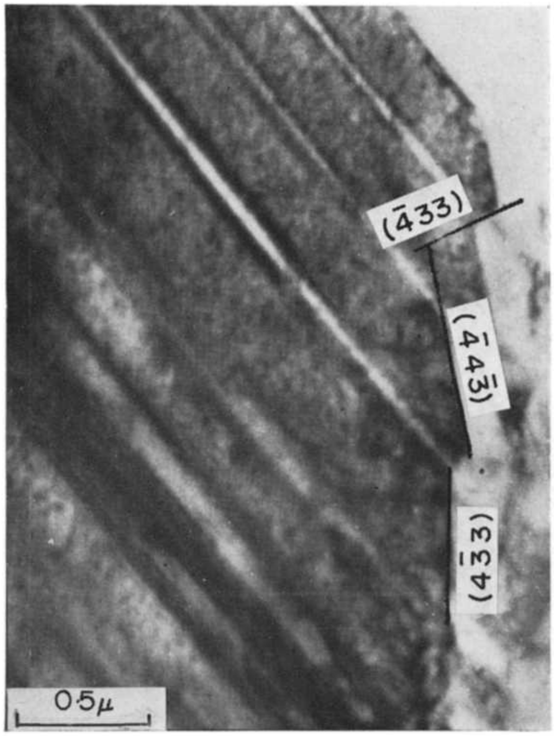

FIG. 14. Martensite of Zr–5.5% Nb alloy showing zig-zag habit plane.

distinctly observable when the twins are thick. It is to be seen from the micrograph that each twin orientation has its own plane interface. Single surface trace analysis has shown that the average habit plane is $(4\bar{3}3)_\beta$, while the habit due to twin intersection on the plate boundary is $(\bar{4}33)_\beta$ and that corresponding to the spacing between twins is $(\bar{4}43)_\beta$.

DISCUSSION

In the present investigation two distinct morphologies of martensite have been noticed confirming earlier observations. Pure zirconium and alloys containing less than 0.8% niobium show colonies of twin free martensite laths stacked parallel to each other. From the lattice parameters of α' and β zirconium and from the Burgers orientation relation, the principal lattice strains can be estimated to be a 2 per cent expansion along $[011]_\beta$, which becomes $[0001]_{\alpha'}$, a 10 per cent expansion along $[01\bar{1}]_\beta$, which becomes $[01\bar{1}0]_{\alpha'}$ and another 10 per cent contraction along $[100]_\beta$ which becomes $[2\bar{1}\bar{1}0]_{\alpha'}$. The expansion along $[011]_\beta$ being small and principal strains along other two axes being positive and negative, the lattice strain itself is close to the invariant plane strain. This means that the lattice invariant strain which will be necessary for the total strain to satisfy the invariant plane strain condition is expected to be small. The absence of any internal twinning in the martensite of pure zirconium and dilute alloys coupled with the large spacing between the internal twins in more concentrated alloys are consistent with this crystallographic prediction. The M_s temperature of pure zirconium being 850°C,[8] the small inhomogeneous shear can take place by a slip with the dislocations at the lath boundary presumably participating in the deformation process. A typical dislocation structure at the lath boundary is observed in the present investigation. Contrast experiments on similar lath boundary of Ti–Cu massive martensite[4] has shown that the Burgers vectoı of such dislocations are of the type $1/3\langle 2\bar{1}\bar{1}3\rangle$. No regular structure of dislocations has been observed inside the laths perhaps due to their rearrangement subsequent to the transformations.

In case of acicular martensite, $\{10\bar{1}1\}$ twinning is the predominant mode of inhomogeneous shear. The internal twinning in these alloys, is generally quite uniform. Concentration of twinning along the central line or midrib of the martensite plate is not observed, which points out that once twins are nucleated during the initial stages of formation of martensite plate, they continue to grow in length as the martensite plate thickens. The mode of inhomogeneous shear remains unchanged during the process of growth of the plates.

According to the phenomenological theory, the habit plane is an undistorted plane only on a macroscopic scale. For a twinned plate, it has been observed that the habit interface is constituted of many twin interface widths. If it is assumed that the inhomogeneous shear occurs only on twin plane alone, then the strain inside a twin will be purely a lattice strain. Since the lattice strain is not an invariant plane strain, some amount of distortion along the interface will be present. Hammond and Kelly[5] postulated that these small scale distortions are minimised by occurrence of a series of dilatation which makes the lattice strain at each twin interface an invariant plane strain. These dilatations cancel out on the macroscopic scale since they act in opposite sense across each interface. In the present investigation definitive evidence of microscopic lattice invariant shear inside the twins has been noticed. Inside each $(10\bar{1}1)$ twin band, the straight and regular arrangement of dislocations on $(01\bar{1}1)$ planes are caused by a slip shear along that plane. The direction of shear on $(01\bar{1}1)$ plane being $[11\bar{2}\bar{3}]$, the second lattice invariant shear can be accommodated completely by the transformation twins associated with the first one. This combination of shears satisfies Cahn's continuity condition[9] which requires that the shear direction of the second shear be parallel to the shear plane of the first shear. This mechanism of multiple shear lattice invariant deformation points out that the strain inside each twin band consists of both strains corresponding to lattice deformation and lattice invariant deformation. Without introduction of dilatation along the interface of individual twins, this mechanism is able to explain the plane strain condition along the interface of each twin. The individual twin interface in the present alloy system has also been shown to lie along $\{334\}_\beta$ and $\{344\}_\beta$ type planes, similar to but not identical with Hammond and Kelly's work on titanium–manganese martensite. Otte[10] has shown that for $\{334\}_\beta$ and $\{344\}_\beta$ martensitic transformation in Ti and its alloys, the most likely shear system is $(\bar{1}011)[2\bar{1}\bar{1}3]$ slip. The same shear system appears to be operative inside a twin band.

Another type of multiple shear inhomogeneous deformation has been observed which shows $(2\bar{1}\bar{1}2)$ twins intersecting with dislocations lying on $(1\bar{1}01)$ plane. In this case the dislocations are not accommodated inside the transformation twin bands as it has been observed in the earlier case. The dislocations are running across the twin–matrix interface without any noticeable deviation in their direction. This observation can be explained by a multiple shear taking place on $(2\bar{1}\bar{1}2)$ plane and $(1\bar{1}01)$ plane by twin and slip, respectively, along their common direction $[2\bar{1}\bar{1}\bar{3}]$. From the geometry of the twinnned hexagonal crystal, Yoo[11] has listed the possible slips that can take place across some of their common twin planes. From his analysis the present observation is a valid one. The dislocations remain undeviated because the $(1\bar{1}01)$ of matrix orientation is coplanar with an equivalent plane $(10\bar{1}1)$ of the twin orientation. Incidentally this multiple shear consists both the slip systems which Otte[10] has referred to as the most likely slip systems involved in the martensitic transformation of titanium and its alloys.

Like many other alloy systems, the transition from the slipped to twinned martensite in these alloys appears to be related with the M_s temperature. As the transformation temperature goes down with increasing addition of niobium in zirconium,[8] twinning, which is a more favourable mode of deformation at relatively lower temperature, takes place predominantly. This results in increasing the fraction of the total number of plates, that are twinned. It is to be noticed that all the plates are not twinned in any of these alloys. In fact, for the alloys containing 0.8–2.3 wt.% niobium, only the primary plates are twinned. The fact that twinning occurs only in the plates which are formed fiıst, at temperatures close to the M_s temperature, and not in the secondary plates formed at relatively lower temperatures, suggests that M_s temperature alone is not the determining factor in the selection of the mode of inhomogeneous shear. In general the twinned primary martensite plates are much larger in size than the secondary plates and appear to be formed at a faster rate. It is possible that the rate of migration of interface between martensite and the parent phase plays an important role in determining the mode of shear, a faster rate facilitating twin nucleation.

Optical metallographic observation of the structure of martensite has indicated that the number of plates formed per unit volume of parent β is much more in case of acicular structure compared to that in massive morphology. The transition in morphology thus can be attributed to the number of embryos per unit β volume actually participating in the transformation. It has already been pointed out that the massive morphology results from nucleation of plates having the same variant of orientation and their subsequent growth, as against secondary nucleation of plates predominating over growth of primary plates in acicular martensite. This observation leads again to the general conclusion namely the massive martensite is a nucleation limited process while the acicular one is a growth limited phenomena.

Gaunt and Christian reported the habit plane of martensite of pure zirconium, from trace analysis of surface relief markings to be very near to $\{334\}_\beta$ plane. Similar surface relief markings have been utilised by Williams *et al.*[12] to conclude that habit of massive martensite of pure titanium lies close to $\{334\}_\beta$. The present investigation in which the determination of habit plane has been worked out from the trace analysis of the lath boundary also indicates that the habit plane is close to the $\{334\}_\beta$ plane. This confirms that the surface relief markings observed in the massive martensites of zirconium or titanium, actually correspond to the lath boundaries. But this observation goes against that of Willaims *et al.* on Ti–Cu martensites, in which the interface boundary was reported to be parallel to $\{10\bar{1}1\}_{\alpha'}$ plane. Working backwards through the Burgers' relations not a single $\{10\bar{1}1\}_{\alpha'}$ plane can be coincided even approximately with $\{334\}_\beta$ planes. Thus they suggested a mechanism based on rotation of the lath boundary subsequent to the transformation. However, such an ambiguity did not arise in the present studies. The habit plane of the martensite found in zirconium–niobium alloys appear to have no relation with the concentration of niobium. This is to be expected because the principal lattice strains do not change significantly with change in niobium content. The principal lattice strains are a/a_0, $(\sqrt{3/2})\ (a/a_0)$ and $1/\sqrt{2}\,\gamma(a/a_0)$ where a_0 is the cubic lattice parameter, a and c are the hexagonal lattice parameters and $\gamma = c/a$, and they do not alter appreciably as the ratios of a/a_0 and c/a (Table 1) are not influenced by the niobium content. A rather large dilatation parameter of about 1.5 per cent, obtained by plotting the experimental habit plane on the Bowles–Mackenzie net, stands in the way of satisfactory explanation of the present transformation with B and M theory. The theory based on $\{10\bar{1}1\}$ twinning has considered only one system of inhomogeneous shear but the present experiments have shown the existence of more than one system of shear taking part in the lattice invariant deformation. The more recent generalised theories of martensitic transformation[13,14] may perhaps be able to explain the martensitic transformation of zirconium and its alloys more accurately without introducing dilatation.

CONCLUSIONS

Pure zirconium and zirconium alloys containing up to 5 wt.% niobium, when quenched from the beta phase, exhibit a martensitic transformation. The details of the observations can be listed as follows:

1. Pure zirconium and alloys containing up to 0.8% Nb, show a massive morphology with no internal twinning within the plates.

2. Alloys containing greater than 0.8% Nb show an acicular martensite with internal twinning on $\{10\bar{1}1\}$ planes.

3. The primary platelets in the acicular structure are found to be internally twinned, while the secondary are not. The number of platelets that are twinned also increases with increasing niobium content.

4. Habit plane remains unaltered with the addition of niobium.

5. It is found that more than one lattice invariant shear is operating in the alloys studied here. Twinning on $\{10\bar{1}1\}$ and $\{11\bar{2}2\}$ and slip on $\{10\bar{1}1\}$ are the observed shear systems.

ACKNOWLEDGEMENTS

The authors would like to thank Dr. M. K. Asundi, Head, Physical Metallurgy Section and Prof. P. R. Dhar of the Indian Institute of Technology, Kharagpur for many valuable suggestions. Thanks are due to Mr. S. J. Vijayakar and Mr. G. E. Prasad for their co-operation during the course of this investigation. They are also grateful to Dr. V. K. Moorthy, Head Metallurgy Division for his keen interest in the work and for permission to publish this work.

REFERENCES

1. C. D. Williams and R. W. Gilbert, *Trans. Japan Inst. Metals* **9,** Suppl., 625 (1968).
2. G. T. Higgins and E. Banks, Special Report No. 93, Iron and Steel Institute, London (1966).
3. W. G. Burgers, *Physica* **1,** 561 (1934).
4. J. C. Williams, R. Taggart and D. H. Polonis, *Metall. Trans.* **1,** 2265 (1970).
5. C. Hammond and P. M. Kelly, *The Science Technology and Application of Titanium*. Pergamon (1970).
6. J. K. Mackenzie and J. S. Bowles, *Acta Met.* **5,** 137 (1957).
7. P. Gaunt and J. W. Christian, *Acta Met.* **7,** 534 (1959).
8. D. L. Douglass, *Atomic Energy Review*. Vol. 1, No. 4, p. 71 (1963).
9. R. W. Cahn, *Acta Met.* **10,** 113 (1962).
10. H. M. Otte, *The Science Technology and Application of Titanium*. Pergamon (1970).
11. M. H. Yoo, *Trans. Am. Inst. Min. Engrs* **245,** 2051 (1969).
12. A. J. Williams, R. W. Cahn and C. S. Barrett, *Acta Met.* **2,** 117 (1954).
13. A. G. Crocker, *Acta Met.* **13,** 815 (1965).
14. A. F. Acton and M. Bevis, *Mat. Sci. Engr* **5,** 19 (1969/70).